Available online at www.eccomasproceedia.org
Eccomas Proceedia COMPDYN (2023) 592-617

ECCOMAS
Proceedia

COMPDYN 2023
9th ECCOMAS Thematic Conference on
Computational Methods in Structural Dynamics and Earthquake Engineering
M. Papadrakakis, M. Fragiadakis (eds.)
Athens, Greece, 12-14 June 2023

LIMIT-STATE RESPONSE OF STONE MASONRY USED IN THE CONSTRUCTION OF CULTURAL HERITAGE IN GREECE

George C. Manos[1], Kostas Katakalos[2], Lambros Kotoulas[3], Lazaros Melidis[4]

[1,2,3,4,] Lab. Strength of Materials and Structures, Aristotle University
gcmanos@civil.auth.gr, kkatakal@civil.auth.gr, lpkotoulas@gmail.com, lazmelidis@gmail.com,

Abstract

The behaviour of stone masonry structures, without or with mortar joints, forming cultural heritage structures in Greece is presented, especially when they are subjected to earthquake ground motions. Ancient Greek Temples built with dry-fit stones formed in perfect geometry and simply laid on top to each other are examined. When these structures are subjected to seismic loads they develop large displacement non-linear sliding and rocking response. These response mechanisms are studied through an experimental investigation with results utilized to validate relevant numerical predictions. The manuscript also includes simple triplet and diagonal compression tests of stone masonry specimens with mortar joints, to examine their in-plane limit-state behaviour. These results are also used to validate numerical micro-models aimed to realistically predict the behaviour of structural elements, built with stone masonry and mortar joints, under in-plane state of stress which arises when subjected to seismic forces. The non-linear numerical tools resulted in reasonably good agreement for both the stone masonry with or without mortar joints. Finally, a simplified methodology is presented using linear elastic seismic analysis towards simulating numerically the whole structure employing criteria based on specific limit states, which have long been established for stone masonry with mortar joints. Good correlation is observed when predictions are compared with actual structural damage.

Keywords: Stone masonry, ancient Greek Temples, Christian Greek churches, sliding or rocking response, triplet tests, diagonal compression, non-linear numerical analysis, simplified elastic seismic analysis.

ISSN:2623-3347
Peer-review under responsibility of the organizing committee of COMPDYN 2023.
doi: 10.7712/120123.10422.20885

1. INTRODUCTION

Stone masonry has been used in the Easter Mediterranean region for many centuries all the way to prehistoric times. Initially the construction of important structures (Temples, Fortifications etc.) the use of stone masonry proceeded with the continuous development of techniques in forming the stones in shape that could insure a perfect dry-fit condition without the use of any connecting material (mortar). This dry-fit stone masonry construction produced structures that were among the wonders of the ancient world, like the Temple of Artemis at Ephesos, the Mausoleum at Halicarnassus, the Parthenon of the Acropolis at Athens, etc. This type of construction used stones shaped in perfect geometry in a way that by simply laying the various components on top of each other to form columns, colonnades, walls, epistyles and other connecting elements in order to compose the 3-D structure. This type of construction was gradually replaced during the Roman era by introducing mortars with physical properties capable to built structural components that could form impressive structural systems of large dimensions utilizing architectural forms of various shapes (arches, vaults. domes etc.) Initially, multi-story reinforced concrete structures tried to introduce a degree of seismic resistance not without specific problems [1]. Current seismic-resistant design relies on the ability of structural members and their connections to sustain high plastic deformations; however, this did not represent the construction philosophy of stone masonry structure, as will be explained.

1.1. Stone masonry in a dry fit construction.

In figure 1 one celebrated example of dry-fit stone masonry construction is shown, using white marble, as it survives today 2500 years after its construction in the Acropolis of Athens. The structural system is composed of a number of columns and vertical walls being formed from numerous parts having been shaped in a perfect fit geometry. Marble parts are next used to form the horizontal beams (epistyles) bridging the spaces between walls and columns and the top parts form the frieze and the pediments. Finally, a wooden roof at the top shapes the necessary sacred closed space that only very few people could enter.

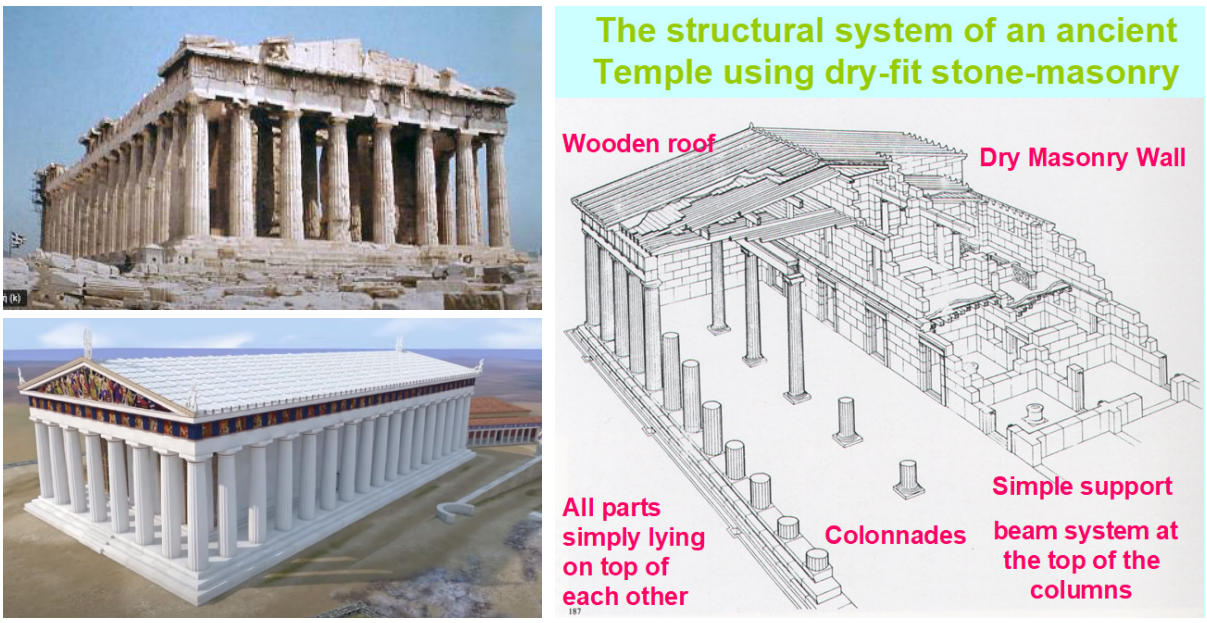

Fig. 1. The structural system of the Parthenon at the Acropolis of Athens using dry-fit stone masonry.

Despite the difficulty is shaping all these parts in perfect geometry this type of construction they could transfer the considerable dead weight of the various parts quite satisfactorily due the dimensions and the compressive strength of stone. The same holds for extreme actions such as wind or snowfall. Seismic excitations are a different extreme action that poses special consideration.

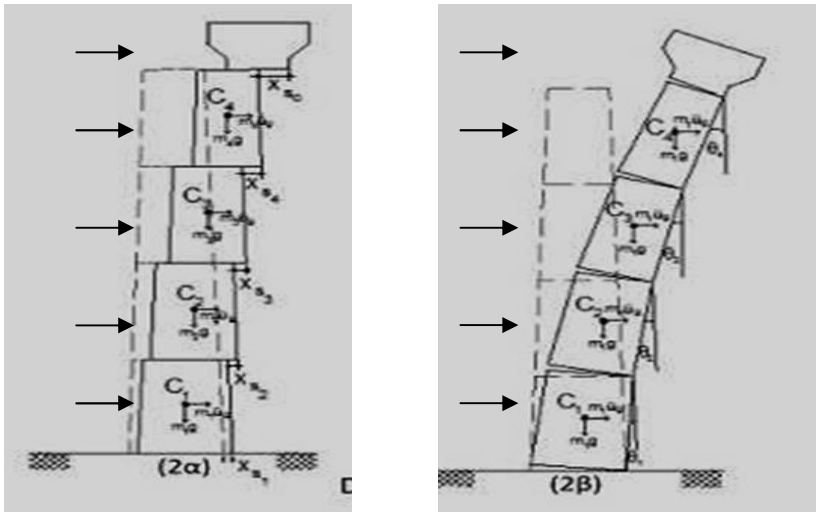

Fig. 2. Simplified sketch of potential sliding or rocking response at the contact surfaces of a Doric column.

When such a structural system is subjected to horizontal seismic ground motions the considerable mass of the various parts leads to seismic forces being generated at all these parts some of the located at considerable height. The fact that all these parts are simply laid on top of each other leads to the following geometric non-linear mechanisms when at the contact surfaces the resisting capacities are exceeded by the relevant demands. This is depicted in figure 2 for a column including 4 drums and its capital at the top ([2] to [9]). At the left the possibility of sliding at the five contact surfaces is indicated whereas at the right the rocking response relatively to five poles is also shown. The stability criteria of these two specific response mechanisms, when they are mobilized, are quite different than those accepted for contemporary structural systems built by either steel or concrete whereby plastic response at predetermined locations of the various structural elements forms the basis of current seismic design. For the depicted structural members the magnitude of seismic forces is limited by the initiation of either the sliding or the rocking response of both. The stability criteria are then linked with acceptable upper limits for either the peak sliding displacements or the peak rocking angles; when these are exceeded partial or total collapse is expected to occur. When the various parts are responding in this way it is reasonable to assume that the state of stress and strain within their volume remains at low elastic levels and they can be ignored when compared with the amplitude resulting from the indicated in figure 2 sliding or rocking response. This description of the stability criteria based on the large displacements is easily understood in terms of rigid body equilibrium conditions; however, it needs to be quantified considering the dynamic nature of the seismic forces and the corresponding sliding or the

settlement of the foundation which is caused by long term or short term deformations of the underlying soil or rock layers. The ability of the various parts to develop relative displacements at the numerous contact surfaces prohibits the development of high stresses in these parts leading again to the upper limit stability displacement criteria mentioned before. It must be underlined here that these large displacements, unless the lead to partial collapse, can be repaired by repositioning the various parts in the original place with not so great difficulty. Similarly, even for the partially collapsed parts the repair and repositioning is relatively easier than the masonry structures built with mortar joints as described in 1.2.

1.2. Structures built with stone masonry built with mortar joints.

These structures are using stones that are shaped in not perfect fir geometry. The various parts are laid on top of each other with the help of very deformable mortar which matures by becoming hard and with increase strength properties after sometime. The stone materials are not selected to be of high compressive strength neither the cross-section of the various structural members is built with the same care. Usually, the two facades are built with more-or-less regularly shaped stone where their core are filled in a very irregular manner. This facilitates the construction and the relative decrease in compressive strength for the various structural elements is compensated by an empirical increase in dimensions. The shape of the stone is more regular for the construction of arches, vaults, and domes etc. which are usually built with great care. Again, the transfer of vertical forces can be performed quite satisfactorily as is usually the case for wind and snowfall. However, the performance of these structural systems under strong seismic ground motions leads to various forms of structural damage and in many cases this can also lead to partial or total collapse ([1] and [10] to [14]). The mortar joints, which facilitated the construction, represent the weak link when these structural elements are subjected to demands generated from seismic excitations. The stiffness and the rigidity of structures built by stone masonry with mortar joints leads to high amplitude seismic forces. Many times, when such structural damage develops, the absence of a perfect fit geometry, such as the ancient Greek temples, does not allow any stable sliding or rocking response. Therefore, the brittle modes of failure of structural elements built with stone masonry and mortar joints can be followed by partial or total collapse of the structural system. It must be underlined that the severe damage and partial collapse usually results structural parts that most of the time cannot be reused. Moreover, the repair and reconstruction effort is many times more difficult than the original construction of the virgin structure. The stiffness and the rigidity of the structural system as a whole are also susceptible to the appearance of structural damage from foundation settlement. This is described in section 3.

2. THE SLIDING RESPONSE OF A PRISMATIC DRUMS

The experimental arrangement of studying the sliding response between two prismatic stone drums lying on top of each other is shown in figure 3 with the bottom one rigidly attached at the strong reaction floor. These monoliths were part of the scheme to restore the fortifications of the Macedonian Palace at Vergina-Greece. The contact surface of this bottom monolith is shown in figure 3b which in perfect fit to a similar contact surface of the top monolith. In figure 3c the added dead load on top of the second monolith is shown in order to simulate the compressive stress level normal to the contact sliding surface. The horizontal force was applied by a servo-hydraulic actuator controlling its horizontal displacement amplitude forcing the top monolith to slide relatively to the bottom monolith. The added dead

load resulted in equivalent uniform compressive stress amplitude equal to 0.0831MPa. The measured sliding response is shown in figure 3d. From this measurements the friction coefficient was found to be equal to μ=0.72. Information on the sliding response can be found in [15] to [21].

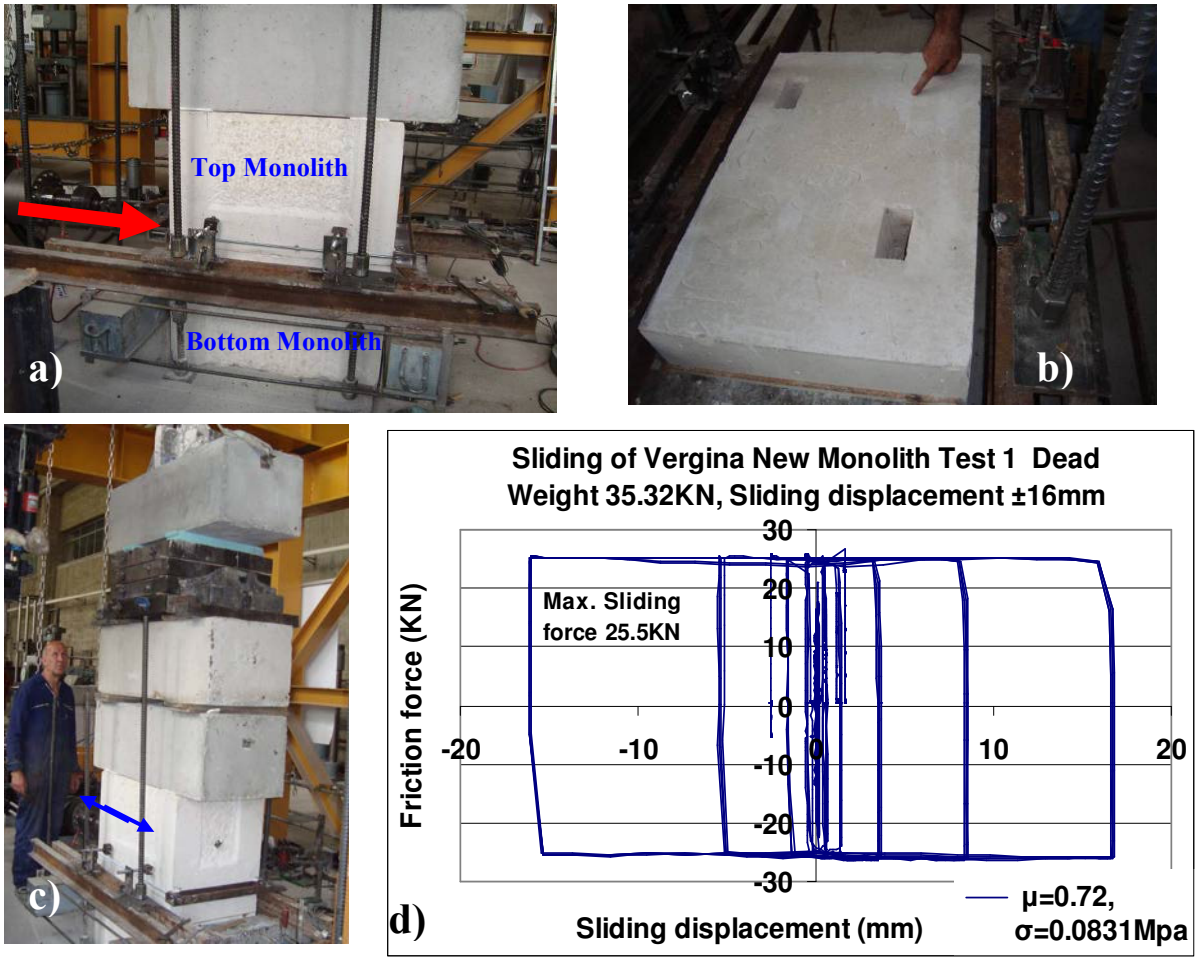

Fig. 3. a) Two monoliths being subjected to sliding response at their contact surface indicated with the red arrow. b) The contact surface of the bottom monolith. c) The experimental arrangement with the sliding direction indicated with the blue arrow. d) Measured sliding response.

2.1. Numerical simulation of the sliding response.

An experimental arrangement similar to the above was used to validate numerical tools aimed to predict the sliding response of two drums lying on top of each other, as depicted in figure 4. The lower drum is rigidly attached to the base-moving platform, so that it can be subjected to the desired base motion of the shaking table, which can also be one-direction horizontal component of a given earthquake recording. The equations of motion were used to create software capable of predicting numerically the sliding response ([20] and [21]). This software was validated by applying it to numerous measurements obtained from the experimental arrangement depicted in figure 4a. Such a comparison between measured and numerically predicted sliding response is depicted in figures 4b and 4c. Figure 4b depicts the measured acceleration of the base motion which was used in this identical form as input

motion for this software. In the same figure the acceleration response of the sliding upper drum is also plotted as it was measured during the experimental sequence and as it was numerically predicted, showing good agreement. The comparison between measured and numerically predicted sliding displacement response is shown in figure 4c exhibiting reasonable good agreement.

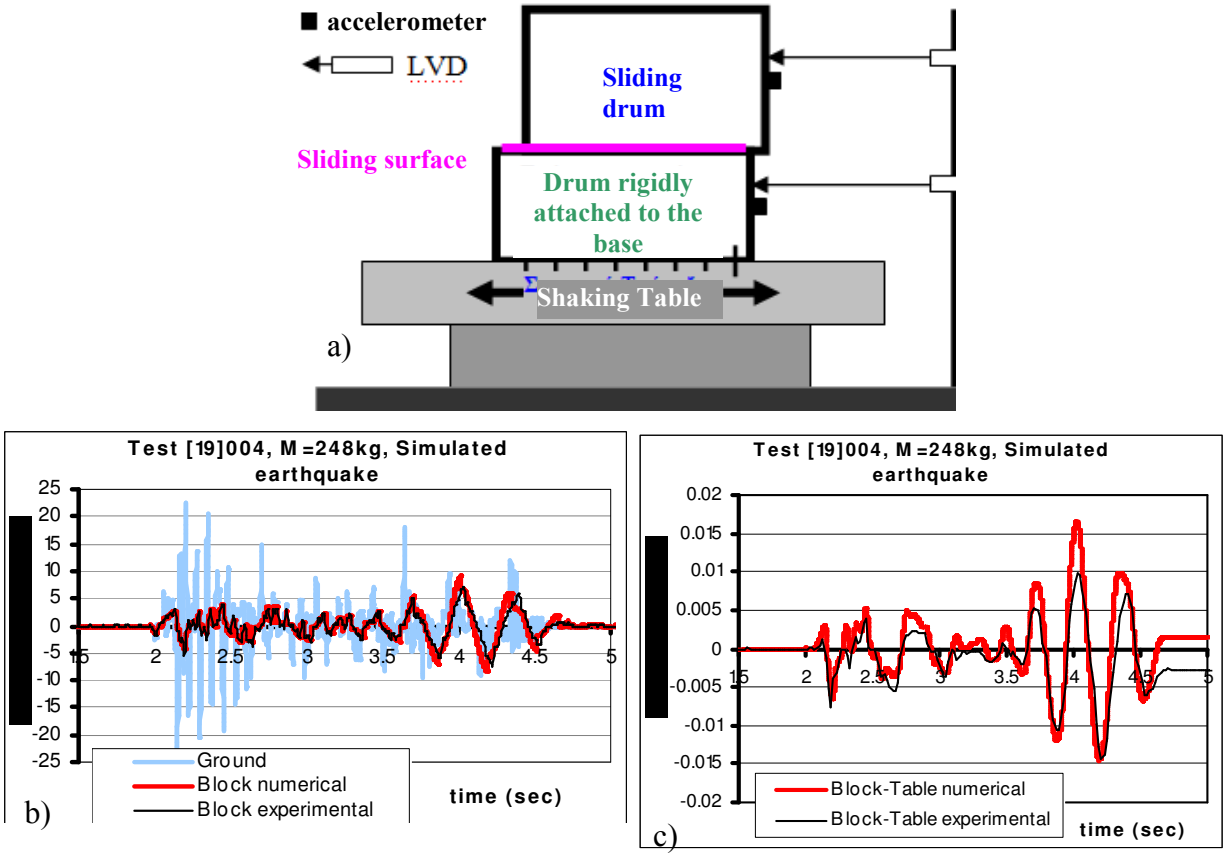

Fig. 4. The sliding response of two drums being subjected to simulated earthquake motions. a) The experimental arrangement with the contact surface of the two drums indicated with the ping arrow b) the measured and predicted acceleration response. c) The measured and predicted sliding displacement response.

3. THE ROCKING RESPONSE OF A PRISMATIC COLUMN

An extensive experimental investigation was performed studying the rocking response of relative slender monolithic columns ([2] and [22] to [29]). They are subjected to one direction horizontal sinusoidal base motions with a frequency which was varied from 1Hz to 7Hz in steps of 1Hz from test to test. This resulted in groups of tests with constant frequency for the horizontal sinusoidal motion for each test. In the various tests belonging to the same group of constant frequency, the amplitude of the excitation was varied progressively from test to test. Figures 4a, 4b and 4c depict the rocking response of the solid specimen during this sequence of tests for three different excitation cases for the same non-dimensional frequency Ω having a value equal to 3.35 (see equation 1). In all cases the monolithic column developed stable rocking response. The response parameter that is plotted in figures 5a to 5c is the ratio of the

rocking angle over the critical angle. For the case of the prismatic specimen the critical angle is equal to 0.1886rad. Moreover, the intensity of the excitation, as expressed by the value of the non-dimensional amplitude A, keeps increasing from the value of 1.05 to the value of 3.35. More information is provided in ([2], [3] and [27].

$$\mathrm{A} = \frac{x}{\theta_{cr} \cdot g}, \qquad \Omega = \frac{\omega}{p}, \qquad p = \sqrt{\frac{W \cdot R_c}{I_o}} \tag{1}$$

A = Non-dimensional base acceleration amplitude
x = Actual horizontal peak base acceleration of the sinusoidal motion
θ_{cr} = Critical angle (rad) indicating overturning of the specimen
g = The gravitational acceleration
Ω = Non-dimensional frequency
ω = Actual sinusoidal frequency (rad/sec)
p = The natural rocking frequency of the specimen (rad/sec)
W = The weight of the block
R_c = The distance of the center of gravity from the rocking pole
I_o = The mass moment of inertia with respect to the rocking pole

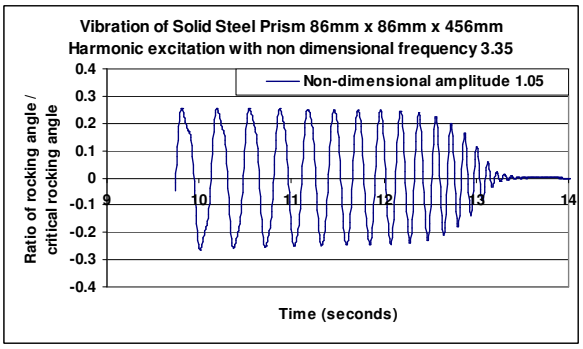

Figure 5b. Rocking response of prismatic specimen for Ω=3.35, A=1.05

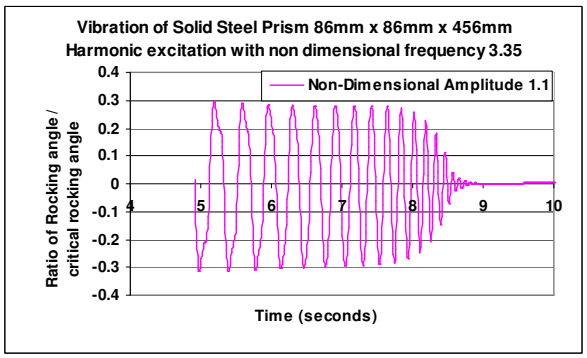

Figure 5b. Rocking response of prismatic specimen for Ω=3.35, A=1.1

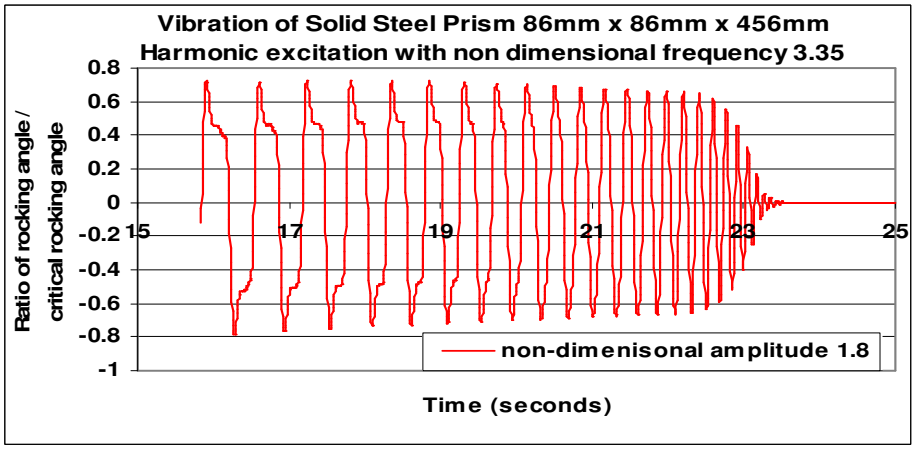

Figure 6c. Rocking response of prismatic specimen for Ω=3.35, A=1.80

All the results from the numerous tests that resulted from the variation of the non-dimensional frequency from 2Hz to 7Hz and the non dimensional amplitude A from 1 to 7 is plotted in figure 6. Keeping the non-dimensional frequency Ω constant and gradually increasing the non-dimensional amplitude A from one test to the next one of the following rocking response mode could develop.

- For small amplitude tests the rocking behaviour is not present; the motion of the specimen in this case follows that of the base.
- As the horizontal base motion is increased in non-dimensional amplitude A, rocking is initiated. This rocking appears to be sub-harmonic in the initial stages and becomes harmonic at the later stages (figures 5a to 5c). This can be denoted as "***stable rocking***" response.
- Further increase in the amplitude of the base motion results in excessive rocking response, which after certain buildup leads to the overturning of the specimen. This can be denoted as ***"unstable rocking"*** response. At this stage, the rocking response is also accompanied by some significant sliding at the base as well as by rotation and rocking response out-of-plane of the excitation axis.

Figure 6 includes the results of all these numerous tests, each one corresponding to a set of non-dimensional frequency value Ω_l and non-dimensional amplitude A_j of the excitation. If the above experiments are repeated with a new constant value of the non-dimensional frequency equal to Ω_i varying again only the non-dimensional amplitude A_k of the excitation a new set of observed rocking response (Ω_i , A_k) will be obtained. For the new set of observed response the comments made before will again be valid. All these sets of observed response (Ω_i , A_k) can be depicted on a plot having as abscissa the non-dimensional frequency value Ω_i and as ordinates the non dimensional amplitude of the base motion A_k. From all these results the ones distinctly plotted are: a) With a purple small circle the tests when from no-rocking the stable rocking response develops. b) With a green small square the tests when from stable rocking is followed by unstable rocking just by a small non-dimensional amplitude increase. Connecting all these limit points with the same meaning together certain boundary lines are formed within figure 6. With these two boundary lines the 2-D space of figure 6 is divided in three regions: a) the "no rocking" region b) the "stable rocking" region and c) the "unstable rocking" region.

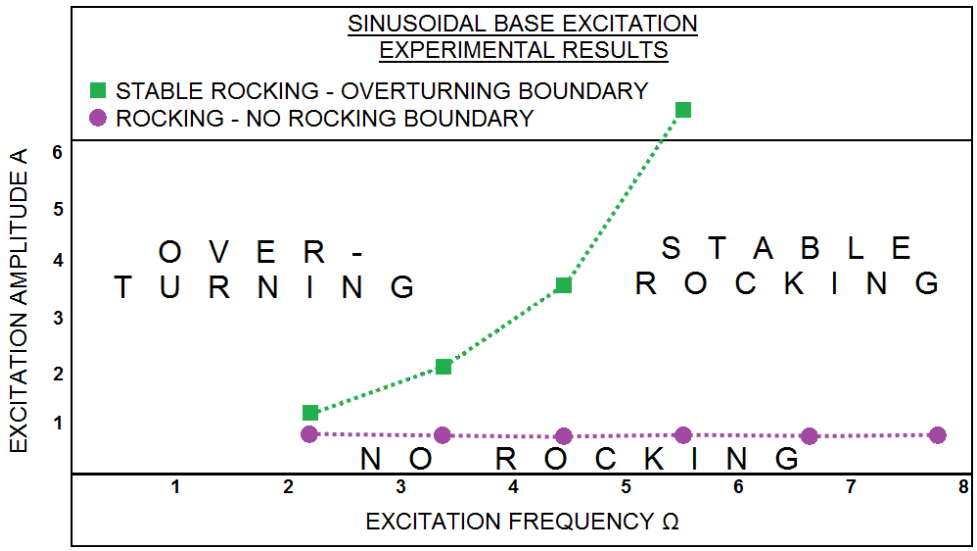

Fig. 6. Mapping the stable-unstable measured rocking response

The following observations summarize the main points of these two boundary lines of figure 5:

- The non-dimensional stable-unstable limit rocking amplitude values A_k increases rapidly with the non-dimensional frequency.
- For small values of the non-dimensional frequency Ω_i the transition stage from no-rocking to overturning, in terms of non-dimensional amplitude value A_k, is very small and it occurs with minor amplitude increase.
- The no-rocking stable rocking non-dimensional amplitude values A_k remain almost constant and equal approximately to one (1) for all non-dimensional frequency values Ω_i.

Apart from the above the following general remarks are also worth stating:

- All the above are results based on dynamic excitation of one dimensional horizontal component. It is obvious that a two horizontal and one vertical component seismic excitation represents a more complex base motion. Moreover, it represents the rocking response of a single colonnade and not a 3-D structural assembly.
- The frequency content of the seismic excitation includes a wide range of frequencies. Despite this, if one is permitted to use qualitatively the observations of figure, intense earthquake activity of relatively large magnitude who reaches large distances with ground motions rich in low frequency (long period) content are expected to be very damaging for this type of structural systems.
- Such earthquakes are relatively rare events and this partly explains how such type structural systems kept being built for many centuries in the ancient world. The destruction of earthquake forces was assisted by a variety of man made actions (wars, religion and social changes, and more recently pollution). Therefore, the current state of ruin can only be counteracted by a long-term effort for their conservation and repair based on sound scientific and technical knowledge.

3.1. Numerical predictions of the rocking response

A considerable number of research efforts have been published in the past dealing with the rocking response predictions of rigid bodies, similar to the rocking response of the monolithic columns of ancient Greek Temples. In what follows the equations of motion were used to formulate software aimed to predict the rocking response of a monolithic prism similar to the one which was examined in this section. The same plotting convention used to present the experimental results in terms of non-dimensional frequency versus non-dimensional amplitude values is also employed to plot the numerical rocking response predictions. More information is included in the bibliography ([2], [28] and [29]). The comparison between measurements and numerical predictions is depicted in figure 7.

In figure 7 the boundary lines between the “no rocking”, “stable rocking” and “unstable rocking” regions are indicated with the pink lines. The results of each numerical solution corresponding to a discrete case of (Ω_i , A_k) is indicated by one specific symbol: “**N** for no rocking”, “**R** for stable rocking” and “**O** for unstable rocking-overturning”. As can be seen there is reasonably good correlation between the experimental and the numerical boundary lines. The boundary between “stable rocking” and “unstable rocking” regions is indicated with twin pink boundary lines. This is due to the fact that within the range of these two lines some of the numerical predictions indicate stable rocking whereas others indicate

overturning. This fact has been observed by a number of researchers and is part of the uncertainty of predicting numerically such a geometrical non-linear dynamic response.

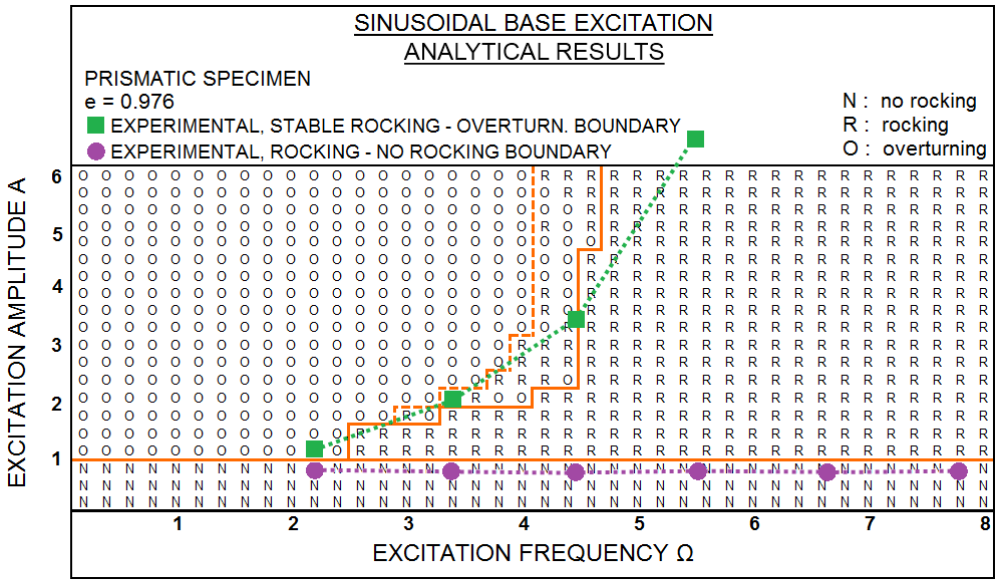

7. Mapping the stable-unstable measured and predicted rocking response

The boundary between “stable rocking” and “unstable rocking” regions is indicated with twin pink boundary lines. This is due to the fact that within the range of these two lines some of the numerical predictions indicate stable rocking whereas others indicate overturning. This fact has been observed by a number of researchers and is part of the uncertainty of predicting numerically such a geometrical non-linear dynamic response. On the side of the physical phenomenon, it must be underlined that such uncertainty is also present due to changes in the way the loss of the kinetic energy is done after every impact of the rocking body to the base takes place. In addition, certain conditions, which may seem insignificant, may play a role when a rocking body is at the verge of other rocking without overturning or rock to its instability. It is obvious, that this phenomenon becomes even more complicated for three component seismic motions and for contact surfaces which, due to various past causes, are far from the ideal full contact conditions usually assumed during the numerical solutions.

4. THE SEISMIC RESPONSE OF STONE-MASONRY WITH MORTAR JOINT CHURCHES

During the last fifty years, various parts of Greece have been subjected to a number of damaging earthquakes ranging from Ms = 5.2 to Ms = 7.2 on the Richter scale. Some of these events, not necessarily the most intense, occurred near urban areas [1]. Numerous Christian churches built with stone masonry with mortar joints were badly affected from this earthquake activity.

a. The Rotunda - Thessaloniki

b. The Rotunda (St. George) Thessaloniki

c. The Achiropiitos - Thessaloniki

d. The Sacred Apostoles – Kalamata

e. Ypapanti - Kalamata

f. Ypapanti - Kalamata

g. Taxiarchon Chromio Kozani

h. The assumption of Virgin Mary Knidi - Grevena

i. St. John the Baptist Lefkovrisi Kozani

j. Taxiarchis – Aeani Kozani

k. Taxiarchis – Aeani Kozani

L The Chatholikon of St. Nikanor Zavorda Grevena

Fig. 8. Typical damage patterns and partial collapse of Christian churches in Greece built with stone masonry with mortar joints.

Figures 8a to 8l depict typical stone masonry churches, damaged by past earthquake in Greece. They include the “Rotunda” and the “Achiropiitos” damaged by the Thessaloniki 1978 earthquake, the “Apostoles” and the “Ypapanti” damaged by the 1986 Kalamata earthquake, and numerous churches (figures) damaged by the Kozani 1995 seismic activity. Two main contributing factors have come to light from investigating this structural damage. The first factor is the pre-existing state of stress and strain either from previous earthquake events and/or from long term permanent foundation settlement [45]. The second factor is the intensity of the seismic ground motion and the earthquake forces generated by it ([1], [12], [13]. [34] and [35]). These observed damage forms are in agreement with typical damage

observed in such structural formations in other countries, with the most pronounced case being the churches damaged by the L' Aquila earthquake ([34] and [35]). The study of this type of performance can have a number of objectives:

- To comprehend the fundamental causes of such damage in order to possibly prevent its appearance by appropriate countermeasures prior to a seismic event.
- To be able to develop appropriate countermeasure for the repair and strengthening after a damaging seismic event.
- To validate effective experimental and numerical tools that can be mobilized in the above tasks.

These objectives are also valid for the case of the Ancient Greek Temples presented before. However, there are a number of complications in both cases depending on the status of each individual structure relevant to its characterization as "Cultural Heritage". This is because there are a number of limitations and conditions that the investigation, the repairs, the interventions and relevant works must conform for Cultural Heritage structures. These complications can also be seen as a challenge for Architects, Engineers and Researches to propose valid intelligent solutions in a multidiscipline effort to devise applicable solutions. Towards this end results from an experimental investigation is presented in 4.1. studying the mechanical properties of stone masonry components when subjected to simple tests. Next, a simplified numerical process is summarized aimed to be utilized as a tool for a preliminary evaluation of a given stone masonry structure of this type.

4.1. The triplet test

One of the main difficulties in assessing the capacity values for old stone masonry construction is the lack of experimentally verified strength values. In order to partially overcome this difficulty a number of specimens were built employing stones with a cubic compressive strength of 60MPa and medium strength mortar with a mean cubic compressive strength equal to 4.50MPa. Each specimen was built with three stones and two mortar joints. Each mortar joints were approximately 20mm. The dimensions of each stone were approximately 160mm x 380mm x 200mm. Each specimen was placed in a testing rig hosting a vertical jack with a load cell and a flat sliding bearing resting at the top surface of each specimen (figure 9). In addition, a horizontal actuator was securely attached at the mid of the central stone in order to apply a horizontal load in a gradually increasing manner, keeping at the same time the vertical load constant at a predetermined level. The aim of this experimental setup was to force each specimen to fail in an almost horizontal sliding mode at either one of the two mortar joints. Two displacement transducers were attached on this specimen at each one of the mortar joints dedicated to capturing the sliding displacement of the central stone relatively to the top and bottom stones. The final objective of such an experimental sequence is to be able to quantify the shear resistance offered by stone-mortar joint which is within a stress field with compressive stresses acting normal to the stone-mortar joint interface. The stone-mortar joint shear resistance involves both the cohesion mechanism between stone and mortar as well as the sliding friction mechanism. The resulting sliding response is depicted in figure 10 including the variation of the recorded horizontal and vertical load, respectively.

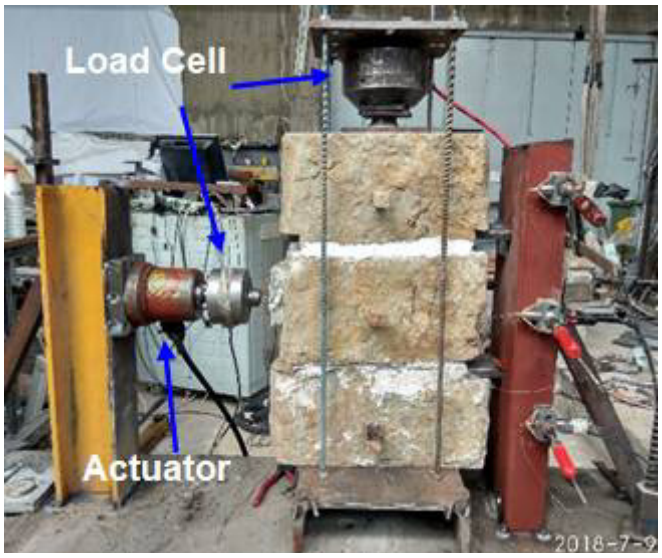

Experimental set-up
of the triplet test

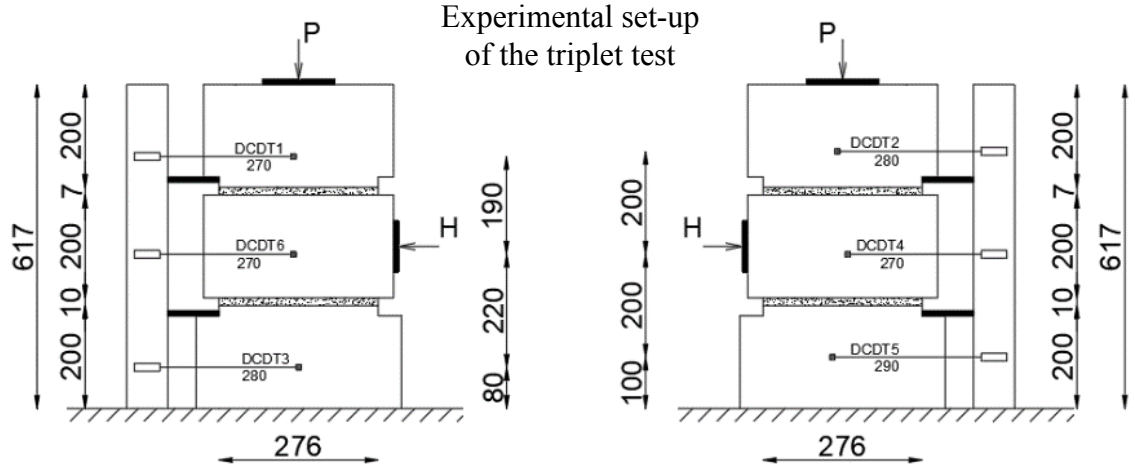

Fig. 9. Triplet test experimental set-up

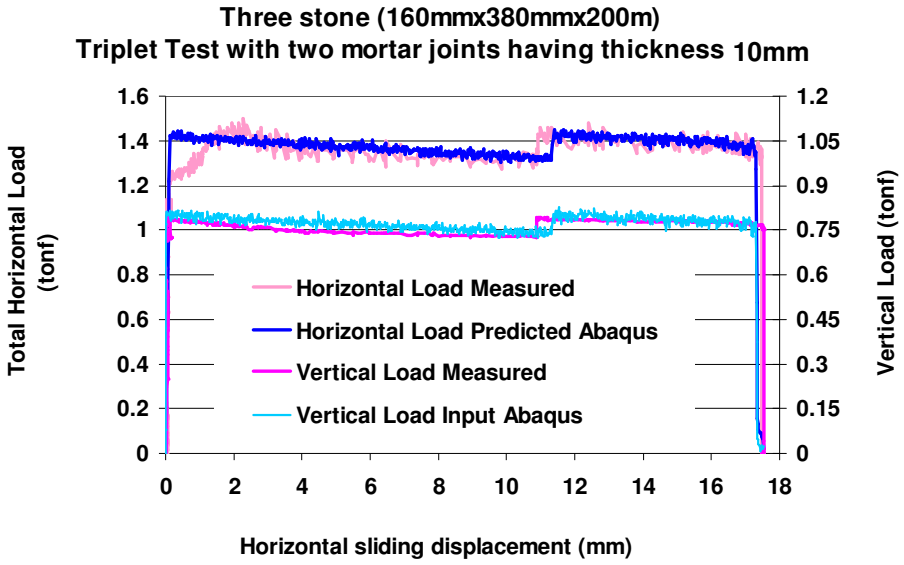

Fig. 10. Comparison of the measured and numerically predicted sliding response of the tested triplet. Friction coefficient μ=0.90 cohesion fvko=0.12MPa.

A numerical model of the performed triplet test was formed [30] assuming that the three stones behave elastically whereas the two mortar joint were provided with non-linear constitutive behaviour. Each mortar joint was numerically simulated with a contact surface joining the two adjacent stones governed by a cohesive surface interaction constitutive law. The most important parameters governing this numerical behaviour are the value of the cohesion as well as the value of the coefficient of friction. In this attempt to simulate numerically the measured triplet response depicted in figure 9 the values of these parameters were varied in a parametric way using the measured response as a level of reference through a back analysis process. This non-linear numerical simulation was performed with a time step-by-step analysis with a very small time step that is adjusted by the software according to convergence requirements. The loading sequence was also varied in time and it included at each time step the measured vertical load, which was applied on the numerical model in the same way as was applied during testing. Together with this vertical load a horizontal displacement was also imposed on the numerical central stone resembling the horizontal load which was applied on the triplet during testing.

In figure 11 a comparison is made between the measured horizontal force horizontal displacement response of the three stone triplet of figure 9 with the corresponding numerical predictions obtained from the numerical simulation described in this section. In the same figure the vertical load measured during the experiment and applied as input in the numerical simulation is also plotted and compared with the vertical reaction that results from the numerical simulation solution. As can be seen in this figure, good agreement is reached between the experimental measurement and the numerical predictions in this case, utilising the back analysis process for choosing the values of the various parameters for the cohesive surface interaction non-linear constitutive law, as previously descibed (friction coefficient μ=0.90 cohesion fvko=0.12MPa.). Based on this comparison, it can be argued that such a cohesive surface interaction constitutive law, with values of its parameters validated through the process of the specific triplet test, can be also employed in forming realistic limit-state criteria for stone masonry elements constructed with stone and mortar of similar mechanical characteristics with the ones employed to constructed the triplet specimens. It is already underlined, that such "realistic" limit-state can be utilized together with the simplified elastic numerical simulation of structural systems in order to reach realistic predictions of their expected performance when these structural systems, like churches, are subjected to gravitational forces or extreme actions. In addition, it can also be argued that such a cohesive surface interaction constitutive law, with values of its parameters validated through the process of the specific triplet test, can also be used in forming more complex non-linear numerical model of structural elements, in an effort to simulating the behaviour of such stone masonry structural elements whereby the shear-sliding response is expected to prevail as the dominant response mechanism.

4.2. The diagonal compression-tension test

A relatively simple loading scheme to study experimentally the in-plane performance of masonry panels is the diagonal compression test, as specified by ASTM E519-15 [31] and by RILEM Technical Recommendations for "Testing and Use of Construction Materials" [32]. Such a diagonal compression test replicates the in-plane state of stress that leads to the formation of diagonal cracking in weak masonry panels, which represents their main limit state. All measurements were used to obtain the performance of each specimen in terms of the variation of the equivalent shear stress (τ_s) versus shear strain (γ) calculated through equations 1 and 2, as is described in ASTM E519-15 [31]. Each specimen was designed to be

tested under diagonal compression along one of its main diagonals having a steel double-corner section at the top and bottom corner of the vertical diagonal of each specimen in order to facilitate the application of the compressive diagonal load (fig. 4).

$\tau_s = (0.707 * P) / [0.5 * (L_1 + L_2) * t]$ (Eq. 1)

$\gamma = |\delta\ell_1| / \ell_1 + |\delta\ell_2| / \ell_2$ (Eq. 2)

Notation: The parameters included in equations 1 and 2 are related to the brick façade and are defined below as shown in figure 4. In the same figure the same parameters for the thermo-insulating façade are also shown with the same accented symbols.

P : the applied vertical load.

L_1 and L_2 : the length of the sides of the wallet as indicated in figure 4.

ℓ_1 and ℓ_2 : the length of the vertical and horizontal diagonals the variation of which is monitored with displacement transducers attached on the brick façade of the wallet as indicated in figure 4.

$\delta\ell_1$ and $\delta\ell_2$: the variation of the relevant lengths ℓ_1 and ℓ_2 as they occur during the variation of the applied load (P).

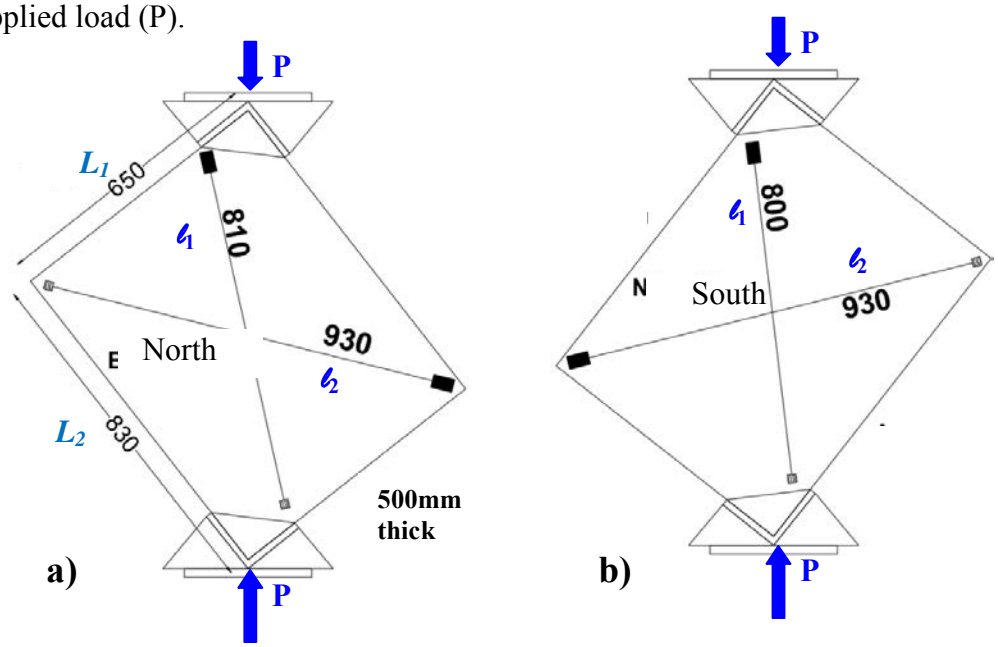

Figure 11: Experimental set up and instrumentation for the diagonal compression test of the stone masonry specimens on façade (a -North) and facade (b - South).

Figure 12 depicts the modes of diagonal dominant cracks which developed during the diagonal compression-tension tests. As can be seen, these cracks go through the mortar joints. This is a typical form of damage for stone masonry with mortar joints of Greek Christian churches which are built with relatively weak mortar. All the material properties of the materials used in the construction of the tested specimens were monitored through out the whole test period. The selected mortar had compositions that could be classified as relatively weak lime mortars that are found as the typical mortars used in this type of stone-masonry construction for Greek Christian churches. The compressive strength of this mortar (with the code name M2) was found to be equal to 4.647MPa whereas the corresponding direct tensile

strength equal to 0.40MPa (found indirectly from tensile strength from flexure utilizing tests of mortar prisms subjected to four point bending).

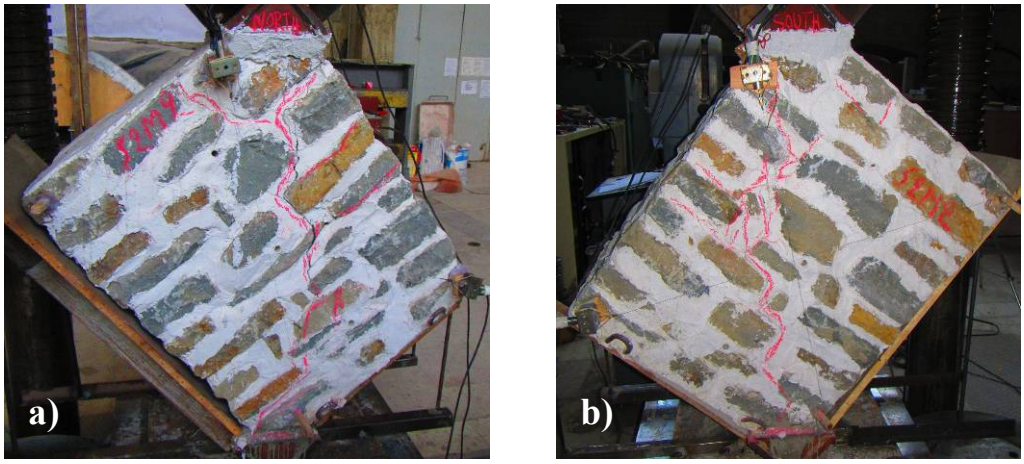

Figure 12: Modes of diagonal cracking during the diagonal compression test of the stone masonry specimens on façade (a -North) and facade (b - South).

The obtained results in terms of -model numerical simulation were utilised together with equations 1 and 2 to obtain the depicted for specimen with code name C4M2 in figure 13. From the linear elastic branch the value of the relevant shear modulus was found to be equal to G=800MPa whereas the maximum value of the measured equivalent shear strength was found to be equal to 0.342MPa.

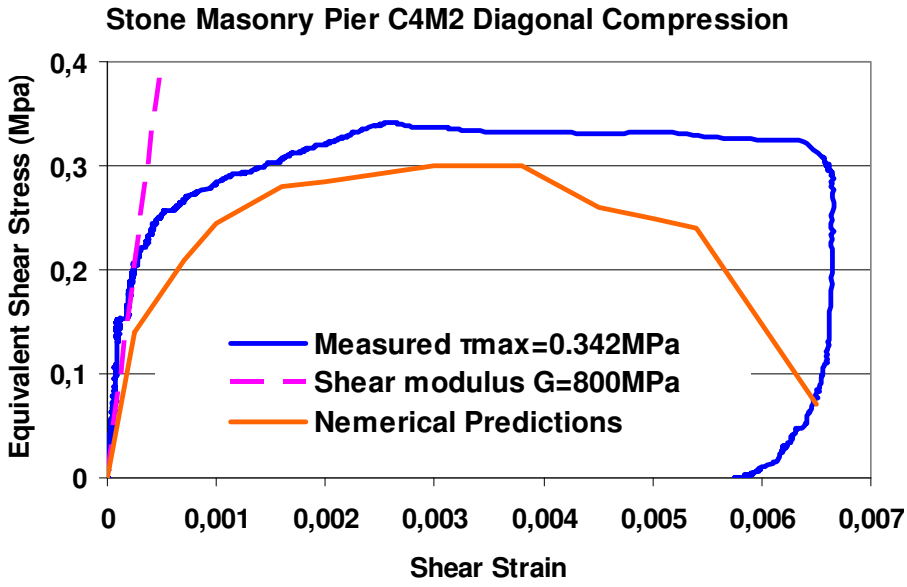

Figure 13. Variation of the equavalent shear stress versus shear strain for stone masonry specimen C4M2 (mortar joints with mortar M2) found from diagonal compression-tension test. Comparison of measured and predicted respone.

Next an attempt was made to simulate numerically this test by employing a micro-modelling process whereby all the stones and the mortar joints were simulated numerically in a discrete way depicted in figure 14. The macro-modelling as well as the micro-modelling was emplopyed in this numerical investigation. Figure 14a presents the employed micro-model using the same numerical methodology that was describe in the numerical simulation

of the triplet test. It was assumed that the all the stones behave elastically whereas all the mortar joint were provided with non-linear constitutive behaviour being numerically simulated with a contact surfaces joining the two adjacent stones. The adopted non-linear constitutive law was governed by a cohesive surface interaction with properties linked with the mechanical properties of the mortar that these mortar joints were constructed with (M2). The resulting variation of the equavalent shear stress versus shear strain is depicted in figure 13.

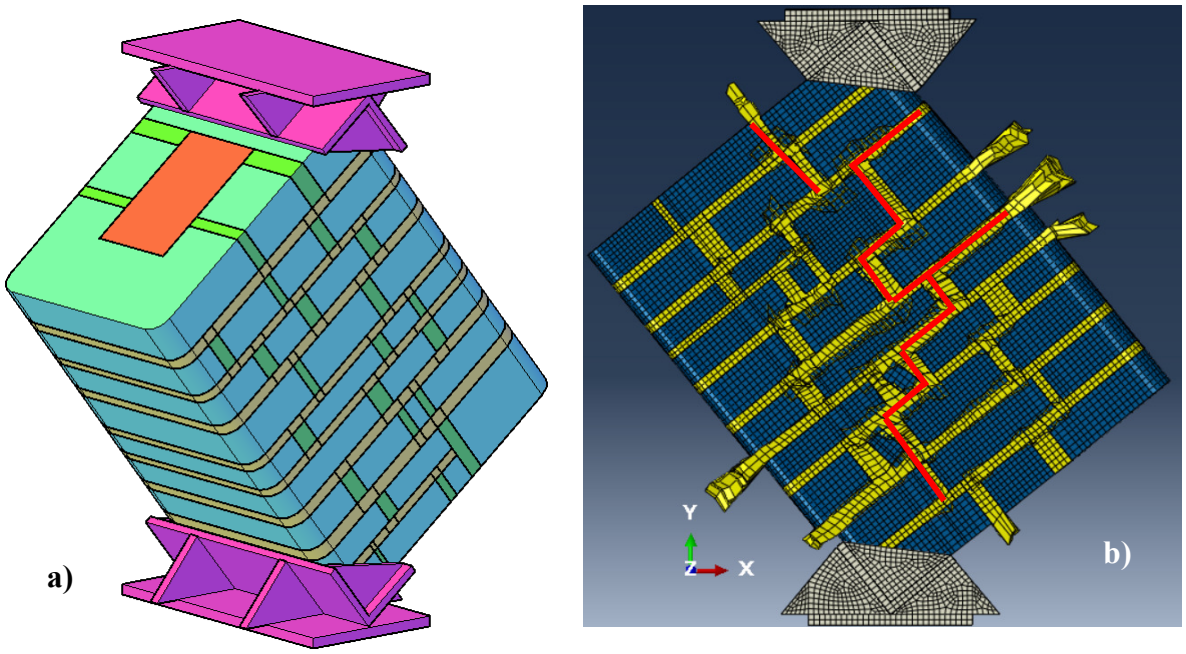

Figure 14. a) The numerical simulation of the diagonal compression-tension test employing micro-modelling. b) Numerical predictions of the observed cracked joints through the regions of large plastic strains.

The numerical applied load and the resulting deformations of this micro-model numerical simulation were utilised to obtain the numerical values of the equivalent shear stress (τ_s) versus shear strain (γ) in exactly the same was as was done during the experiment by applying equations 1 and 2. The numerical simulation included all the details that were employed in applying the compressive load (P) as is shown in figures 11 and 14a. The comparison of the measured and numerically predicted diagonal compression-tension response for specimen C4M2 is shown in figure 13 exhibiting reasonably good agreement. The measured maximum equivalent shear stress value is equal to 0.342MPa whereas the corresponding numerical prediction is equal to 0.30MPa. Figure 14b depicts the numerical predictions of the observed dominant diagonal cracks by pointing out through the red lines the regions of the micro-model whereby the contact surfaces developed large plastic strains. By comparing this predicted "mode of failure" with the observed dominant cracks of figure 12 reasonably good agreement can again be seen. From the above discussion it can be concluded that the non-linear behaviour of stone masonry components built in a way replicating stone masonry construction with mortar joints of Greek Christian churches can be numerically simulated in a reasonable manner in order to predict the usual shear or diagonal tension limit states that usually develop at the structural members when subjected to seismic actions or foundation settlement. It must be underline that towards this objective a very important step is

the quantification of the non-linear constitutive laws that can be done only through a very thorough investigation of not only the basic material properties but also the behaviour of structural sub-assemblies like the triplets or the wallets which were used for the diagonal compressive-tensile test. The micro-model process is quite demanding in computer memory and time and too complex to be extended for simulating an entire structure. Moreover, one should always employ simpler numerical tools before stepping up to such demanding and complex numerical simulations especially when the validity of such attempts is not first verified as is done here. In the next section the methodology of a relatively simple approach is described whereby the results from a dynamic elastic analysis is combined with limit-state scenario in order to evaluate the performance of stone masonry Greek Christian churches with mortar joints when they are subjected to seismic forces or foundation settlement ([35] and [45]).

5. SIMPLIFIED METHODOLOGY FOR THE EVALUATION OF STONE MASONRY GREEK CHRISTIAN CHURCHES

This simplified methodology obtains the demands for all its structural members by forming an elastic 3-D numerical model simulating all the geometric features and the relevant masses of the structure that is studied, assuming that all the interconnections between the stone masonry structural members themselves or with the roof are in-tact [36]. Furthermore, any cracking from pre-existing state of stress is addressed indirectly in a smeared way by lowering the Young's modulus of the stone masonry members, which is assigned values not for compressive but for predominant shear and flexural behaviour ([37] and [38]). The following steps are then performed.

- The in-plane and out-of plane stiffness of the various structural elements is numerically simulated by studying critically their composition and their boundary conditions.
- A modal analysis is performed followed by a critical examination of the resulting eigen-modes by excluding those that are unrealistic for stone-masonry structures, given the brittle performance of their structural elements and their interconnections. This exclusion is compensated by introducing an appropriate amplification mass participation coefficient for the eigen-modes that are retained.

- The 3-D numerical model formed in this way is subjected to seismic action, as defined by the Greek seismic code [39] for the design ground acceleration and Euro-Code 8 for the shape of the design spectrum. The value of q=1.5 is adopted for the response modification coefficient presuming that the analyzed structures are composed of unreinforced stone masonry. The demands (S_{Edi}) are next found from load combinations which include the design permanent loads and the seismic actions performing a dynamic modal analysis. When a specific seismic ground motion recording is available use is made of the corresponding inelastic response spectrum for ductility value equal to μ=1.5. ([40]). From examining the obtained stress response the potentially critical cross sections are identified.
- The capacities (S_{Rdi}) are the found for each critical cross section considering all the possible limit state scenarios depicted in figure .

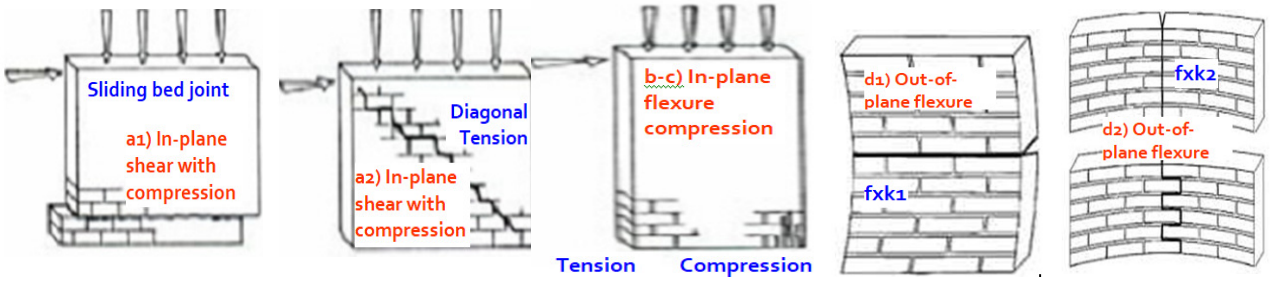

Fig. 15. Five distinct limit state scenarios for structural elements built by stone masonry with mortar joints. The first three are for the in-plane and the other two for out-of-plane states of stress.

In order to estimate the performance of each masonry structural element the following inequalities are employed:

$$R_i = S_{Rdi} / S_{Edi} > 1 \quad \text{no damage} \qquad (3)$$

or

$$R_i = S_{Rdi} / S_{Edi} < 1 \quad \text{structural damage} \qquad (4)$$

S_{Edi} represents the demand posed for each masonry structural element as it results from the simplified numerical simulation; S_{Rdi} is the corresponding capacity value which is obtained on the basis of assumed strength values for the stone masonry (table 2). Note that no safety coefficients are used in estimating the capacity values at this stage of the evaluation process. Inequality 3 signifies safe structural performance. Inequality 4 denotes that the predicted structural performance exceeds a certain limit state thus signifying the development of structural damage corresponding to the specific limit state that is exceeded. These corresponding capacity over demand ratio (R_i) values are used in this simplified numerical evaluation process; a ratio (R_i) value smaller than 1 indicates that a distinct limit state has been reached leading to the corresponding failure mode. The basic assumption is that the in-plane and out-of-plane state scenarios do not interact. The following five common structural damage scenarios are stated corresponding to five distinct relevant limit-states, as indicated in figure 15, through the relevant ratio values ($R_i = S_{Rdi} / S_{Edi}$). Scenario **a_1)** addresses the in-plane shear limit state which corresponds to a sliding failure mode through the value of the ratio ($R_{\tau sli}$) ; scenario **a_2)** addresses the in-plane shear limit state corresponding to a diagonal tension failure mode ($R_{\tau dia}$). Scenario **b)** corresponds to a compressive mode of failure (R_ς) whereas scenario **c)** corresponds to the in-plane tensile limit state (R_σ). Finally, scenario **d)** corresponds to the out-of-plane tensile limit state (R_M). Both scenario **c)** and scenario **d)** use the f_{xk1} strength value, listed in table 2 column 2.

a_1) $R_{\tau sli}$ = shear strength / shear stress demand. $R_{\tau sli} < 1$ signifies in-plane sliding shear mode of failure

a_2) $R_{\tau dia}$ = shear strength / shear stress demand. $R_{\tau dia} < 1$ signifies in-plane diagonal tension mode of failure.

b) R_ς = compressive strength / compression stress demand. $R_\varsigma < 1$ signifies in-plane compression mode of failure.

c) R_σ = tensile strength / tensile stress demand. $R_\sigma < 1$ signifies tensile mode of failure normal to bed joint (in-plane)

d) R_M = tensile strength / tensile stress demand from out-of-plane flexure. $R_M < 1$ signifies out-of-plane tensile mode of failure normal to bed joint at the extreme fibre.

All masonry parts of the studied structures were examined in terms of in-plane and out-of-plane stress demands posed by the applied load combinations against the corresponding capacities, as these capacities were obtained by applying the "Mohr-Coulomb" criterion of equation 1 or the stone masonry compressive and tensile strength limits listed in Table 2. Ratio values smaller than one ($R_{\tau sli}$, $R_{\tau dia}$, R_{ς}, R_{σ}, R_{M} <1) predict the corresponding limit state condition. As can be seen, this methodology is based on combining numerical stress demands resulting from elastic analyses with limit-state strength values. An alternative approach is to incorporate these limit-state strength values in a non-linear push-over type of analysis ([33] and [34]). As was shown in this study by Manos et al. [33] the above linear-elastic approach is a reasonable approximation of the actual behaviour and of predicting regions of structural damage, being both less complex and time consuming than the corresponding non-linear approach. Manos et al. ([38]) developed a relevant expert system for assessing the various resisting capacities of vertical masonry structural elements. The non-linear response of the stone-masonry is approximated first by introducing the response modification coefficient in the response spectrum before obtaining the demands and by considering for the capacities realistic limit-state scenarios (figure 15).

5.1. Numerical simulation of the earthquake response of a stone masonry church in Kefalonia-Greece

The simplified numerical methodology is applied to predict the dynamic and earthquake response of the 17th century "Basilica" church of St. Marina in Soullaroi, which is located in the island of Kefalonia and was heavily damaged during the 2014 earthquake sequence ([41], [42]). The eigen-periods for the N-S transverse direction translational response are equal to 0.177sec and 0.20sec for the hard and medium soil deformability, respectively. Similarly, the eigen-periods for the E-W longitudinal direction translational response are equal to 0.10sec and 0.12sec for the hard and medium soil deformability, respectively. More information on the dynamic properties of this numerical simulation is given by Manos et al. [42]. The numerical dynamic analyses included the superposition of the gravitational forces with the seismic forces specified on the basis of the ground acceleration that was recorded at two stations during the 3rd February strongest aftershock (GEER-EERI-ATC [41], Papaioannou [43]). The corresponding response curves for the Chavriata recording which is more demanding than the Lixouri ground motion, are shown in figures 16a and 16b for the North-South and East-West directions, respectively.

In each one of these figures the relevant constant ductility spectral curves are depicted for a ductility ratio equal to 1.5, which is assumed to be in line with the value of the response modification factor for unreinforced masonry structures (q=1.5). Moreover, the Type-1 and Type-2 design spectral curves specified according to Euro-Code 8 ([40] to [42]) for design ground acceleration equal to 0.36g (g is the acceleration of gravity), importance factor equal to γ=1, response modification coefficient q=1.5 (for unreinforced masonry) and soil category D. Finally, in each one of these figures the eigen-period values of the main translational eigen-modes in the North-South and East-West direction, as specified above, are also indicated. As can be seen from figures 16a and 16b the acceleration spectral ordinates of the actual strong motion in the North-South direction are more demanding (transverse direction for the church, approximately 1.5g) than the corresponding values in the East-West direction (longitudinal direction for the church , approximately 1.0g).

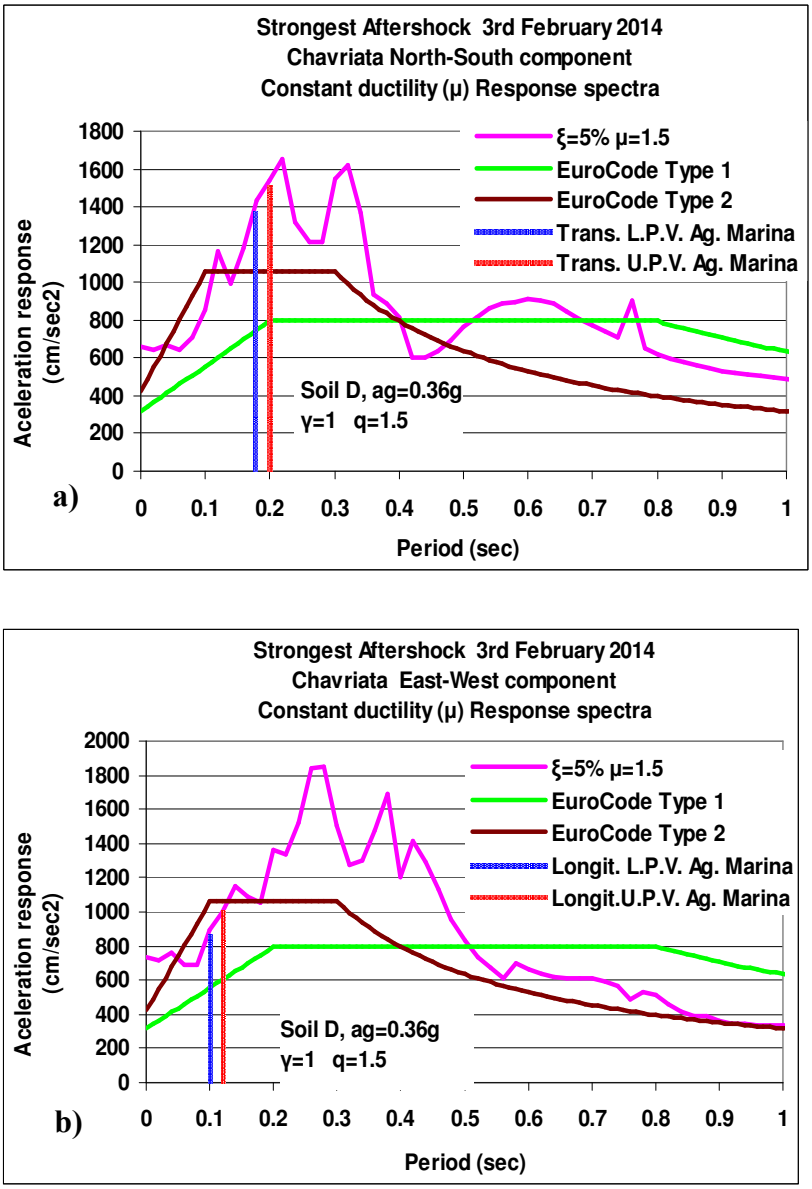

Figure 16. Constant ductility response spectral curves of the Chavriata record, Kefalonia 2014 earthquake together with the relevant Euro-Code 8 design spectral curves: (a) N-S component (b) E-W component.

Such large values of spectral acceleration result in very high seismic load values, listed in table 3 in terms of base shear, that exceed the design seismic loads resulting from applying the Euro-Code 8 provisions for the island of Kefalonia, which belongs to the seismic zone of Greece [39] with the highest expected design earthquake ground acceleration (0.36g). It is no surprising that this old unreinforced stone masonry structure was heavily damaged as was the case for a number of similar structures in nearby locations (Manos et al. [42]).

As can be seen in figure 17 the RM ratio values are well below one (RM < 1) mainly for both North and South longitudinal walls indicating that these walls for this church reached a widespread out-of-plane flexural limit state. Furthermore, this evaluation process indicates that the East and West transverse walls reached at their bottom part in-plane tensile and shear limit states with the corresponding ratio values well below one ($R\sigma < 1$, $R\tau < 1$) whereas at the

top part of these walls the development of the out-of-plane flexure limit state prevails (RM < 1). Again, reasonably good correlation can be seen between predicted limit states, based on the simplified evaluation results of figure 17, with the observed damage shown in figure 18. This simplified methodology can be utilized as a tool for evaluating possible retrofitting schemes [44]. Further non-linear response mechanisms at the corner interconnections and the foundation level are considered for this church in [42] and [45].

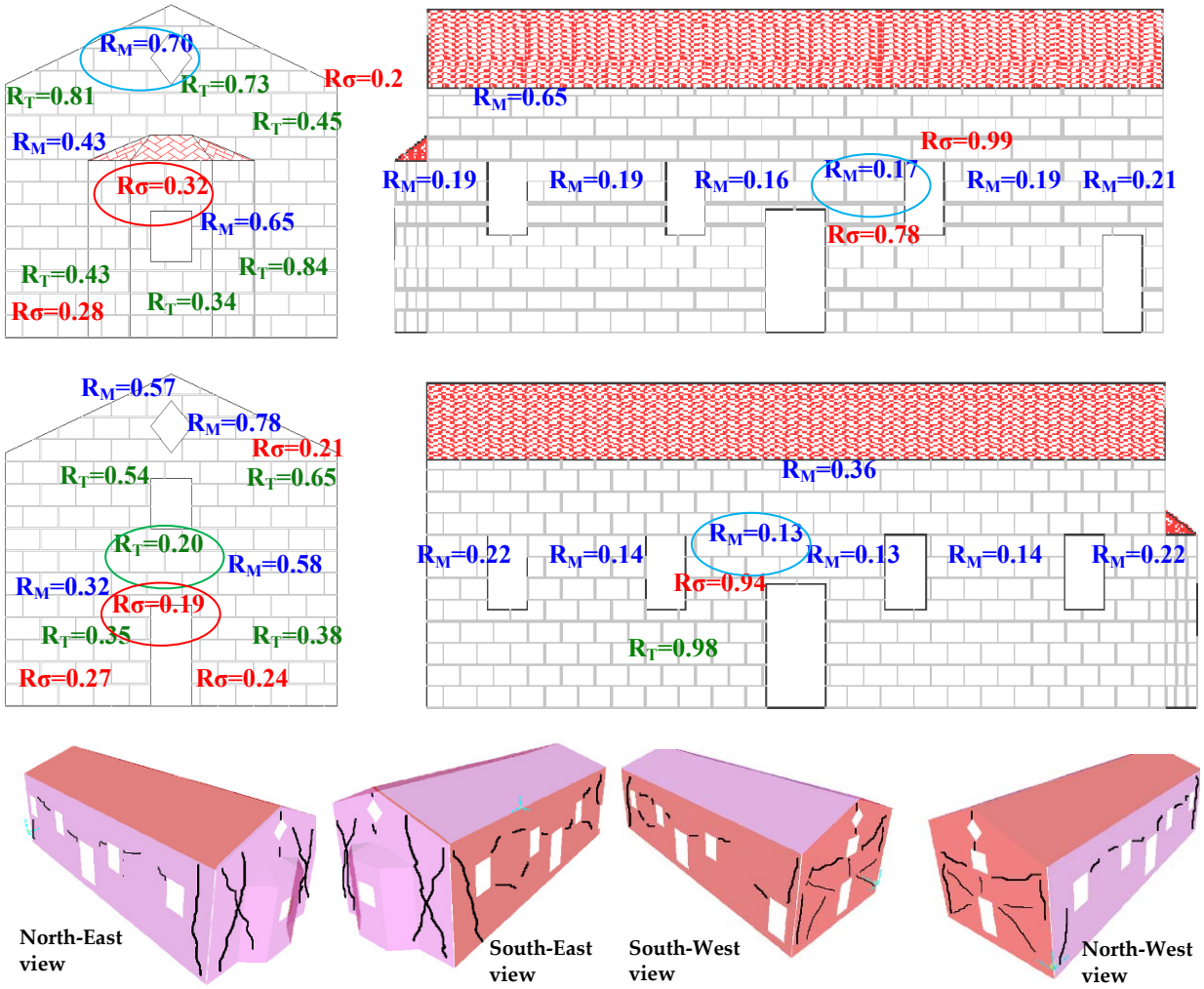

Fig. 18. Summary of observed damage

7 CONCLUSIONS

The behaviour of stone masonry structures, without or with mortar joints, forming cultural heritage structures in Greece is presented, especially when they are subjected to earthquake ground motions. These response mechanisms are studied through an experimental investigation with results utilized to validate relevant numerical predictions. The manuscript also includes simple triplet and diagonal compression tests of stone masonry specimens with mortar joints, to examine their in-plane limit-state behaviour. These results are also used to validate numerical micro-models aimed to realistically predict the behaviour of structural elements, built with stone masonry and mortar joints, under in-plane state of stress which

arises when subjected to seismic forces. The non-linear numerical tools resulted in reasonably good agreement for both the stone masonry with or without mortar joints. Finally, a simplified methodology is presented using linear elastic seismic analysis towards simulating numerically the whole structure employing criteria based on specific limit states, which have long been established for stone masonry with mortar joints.

- Ancient Greek Temples built with dry-fit stones formed in perfect geometry and simply laid on top to each other are examined. When these structures are subjected to seismic loads they develop large displacement non-linear sliding and rocking response. These are large displacement non-linear response mechanisms. Specific experimental arrangements are used to provide results that are use to validate numerical predictions. The obtained measurements are in reasonably good agreement with numerical predictions.
- Christian Greek churches are built with stone masonry with relatively weak mortar joints. Simple experiments with triplets or wallets of such masonry are used to obtain basic information for the in-plane limit state behaviour of such construction. These results are again used to validate numerical tools employing micro-modeling.
- A simplified numerical methodology is presented employing a 3-D simulation of the whole structural system. The basic assumptions are used to simulate realistically the behaviour of such construction to seismic loads or foundation deformability. A linear-elastic seismic analysis is performed aimed to obtain the demands in the structural elements and to identify the critical regions. These are compared with the corresponding capacity obtained by considering specific limit-state scenarios. From the comparison with actual structural damage observed for numerous Christian Greek churches which developed structural damage reasonably good correlations can be seen.

REFERENCES

[1]. Manos G.C., “Consequences on the urban environment in Greece related to the recent intense earthquake activity”, Int. Journal of Civil Engineering and Architecture, Dec. 2011, Volume 5, No. 12 (Serial No. 49), pp. 1065–1090.

[2] Demosthenous M, 1994. Experimental and numerical study of the dynamic response of solid or sliced rigid bodies, Ph. D. Thesis, Dept. of Civil Engineering, Aristotle University of Thessaloniki.

[3] Demosthenous M. and Manos G.C.: "Dynamic Response of Models of Ancient Monuments Subjected to Horizontal Base motions", IABSE, Struct. Preservation of Archit. Heritage, Italy, 1993, pp. 361-368.

[4] G.C. and Demosthenous M.: "Comparative Study of the Global Dynamic behaviour of Solid and Sliced Rigid Bodies", 10ECEE, Vienna, Austria, 1994.

[5] Psycharis, I. N., Papastamatiou, D. Y. and Alexandris, A. (2000) "Parametric Investigation of the Stability of Classical Columns under Harmonic and Earthquake Excitations", Earthquake Engineering and Structural Dynamics, Vol. 29, pp. 1093-1109.

[6] Mouzakis, H., Psycharis, I. N., Papastamatiou, D. Y., Carydis, P. G., Papantonopoulos, C. and Zambas, C. (2002) "Experimental investigation of the earthquake response of a model of a marble classical column", Earthquake Engineering and Structural Dynamics, Vol. 31, pp. 1681-1698.

[7] Papantonopulos, C., Psycharis, I. N., Papastamatiou, D. Y., Lemos, J. V. and Mouzakis, H. (2002) "Numerical Prediction of the Earthquake Response of Classical Columns Us-ing the Distinct Element Method", Earthquake Engineering and Structural Dynamics, Vol. 31, pp. 1699-1717.
[8] Psycharis, I. N., Lemos, J. V., Papastamatiou, D. Y., Zambas, C. and Papantonopoulos, C. (2003) "Numerical Study of the Seismic Behaviour of a Part of the Parthenon Pro-naos", Earthquake Engineering and Structural Dynamics, Vol.32, pp. 2063-2084.
[9] Ambraseys, N. and Psycharis, I. N. (2011), "Earthquake stability of columns and statues", Journal of Earthquake Engineering, Vol. 15, pp. 685-710.
[10]. Binda L., Saisi A., Tiraboschi C., "Investigation procedures for the diagnosis of historic masonries", Construction and Building Materials, Vol.14(4), pp. 199-233, 2000.
[11]. Croci G., "The Conservation and Structural Restoration of Architectural Heritage", Computational Mechanics Publication, 1998, ISBN 1 85312 4826.
[12]. Lagomarsino Sergio "Damage assessment of churches after L'Aquila earthquake (2009)" Bulletin of Earthquake Eng. 2011, DOI 10.1007/s10518-011-9307-x
[13]. Modena C. et al., " L'Aquila 6th April 2009 Earthquake: Emergency and Post-emergency Activities on Cultural Heritage Buildings" Claudio Modena C. et al. , Chapter 20, Earthquake Engineering in Europe, Geotechnical, Geological, and Earthquake Engineering 17, DOI 10.1007/978-90-481-9544-2_20, Springer Science+Business Media B.V. 2010.
[14]. Limoge Schraen C., Giry C., Desprez C., Ragueneau F., "Tools for a large-scale seismic assessment method of masonry cultural heritage", Structural Studies, Repair and Maintenance of Cultural Heritage, STREMAH XIV, WIT press (2015), ISBN 978-1-84564-968-5.
[15] Aslam, M., Godden, W.C., Scalise, L.G., Sliding response of rigid bodies to earthquake motions, Rep. No. LBL-368, Lawrence Berkeley Laboratory, University of California (1975).
[16] Mostaghel, N. Hejazi, M. and Tanbakuchi, J., Response of sliding structures to harmonic support motion, Earthquake Engineering and Structural Dynamics, (11), pp. 355-366, (1983).
[17] Mostaghel, N. Hejazi, M. and Tanbakuchi, J., "Response of sliding structures to earthquake support motion", Earthquake Engineering and Structural Dynamics, (11), pp. 729-748, (1983).
[18] Westermo, B., and Udwadia, F., Periodic response of sliding oscillator system to harmonic excitation, Earthquake. Engineering and Structural Dynamics, (11), pp.135-146, (1983).
[19] Younis C.J. and Tadjbakhsh I.G., Response of sliding rigid structure to base excitation, Engineering Mechanics, ASCE, (110), pp. 417-432, (1984).
[20] Manos, G.C., Koidis, G., and Demosthenous, M., Investigation of the sliding response of a rigid body system subjected to uni-direction horizontal dynamic and earthquake excitations, proceedings 3rd COMPDYN, Corfu, Greece, (2011).
[21] Manos G. C, Koidis G., Demosthenous M., (2013a), "The response of a two-degree-of-freedom dynamic sliding system subjected to uni-direction horizontal dynamic and seismic excitations", Int. J. of Computational Methods and Experimental Measurements, Vol. 1, No. 3, pp.221-237.
[22] Aslam , M.M. et al. 1978. Rocking and Overturning response of rigid bodies to earthquake motions, Report No. LBL-7539, Lawrence Berkeley Lab. Univ. Of California, Berkeley.
[23] Spanos, P.D. and Koh A.S., 1984. Rocking of rigid blocks due to harmonic shaking. J. of Engin. Mech., ASCE 110 (11), pp. 1627-1642
[24] Koh, A.S. and Mustafa G. 1990. Free rocking of cylindrical structures, J. of Eng. Mechanics, Vol. 116, N0 1, pp.35-54.

[25] Shenton, H.W. and Jones, N.P., Base excitation of rigid bodies, I: Formulation, Engineering Mechanics, ASCE, 117(10), pp. 2286-2306, (1991).
[26] Manos, G.C. Reports on Task 1, Task 2 and Task 8, 1998. ISTECH project, Program Environment and Climate, European Commission, Contract No. ENV4-CT95-0106.
[27] Manos G.C., Petalas A., Demosthenous M., (2013a), "Numerical and experimental study of the rocking response of unanchored body to horizontal base excitation", COMPDYN 2013, 12-14 June 2013, Kos Island, Greece.
[28] Manos G.C., Kotoulas L., Melidis L. and Felekidou O. "The Dynamic Response of a Vertical Dry Stone Masonry Wall Mock-up Measurements and Numerical Predictions", 7th ECCOMAS Thematic Conference on Computational Methods in Structural Dynamics and Earthquake Engineering M. Papadrakakis, M. Fragiadakis (eds.), Crete, Greece, 24–26 June 2019.
[29] Manos G.C., Melidis L., Felekidou O. and Katakalos K." The Dynamic Response of a Vertical Dry-Stone Masonry Assembly as a Mock-up of Masonry Wall Fortifications", Proceedings of PROHITECH 2021, Vol. 1 pp. 266-283, Springer, ISBN 978-3-030-90788-4, edited by I. Vayas and F.M. Mazzolani, http://doi.org/10.1007/978-3-030-90788-4.
[30] Hibbitt, Karlsson, Sorensen. Inc. ABAQUS user's manual volumes I–V and ABAQUS CAE manual. Version 6.10.1. Pawtucket, USA; 2010.
[31] ASTM E519-15 (2015) Standard test method for diagonal tension (shear) in masonry, assemblages. American Society for Testing Material
[32] RILEM LUMB6 (1994) Diagonal tensile strength tests of small wall specimens (1991). Rilem recommendations for the testing and use of constructions materials. RILEM, pp 488–489.
[33]. Manos G.C., Soulis V.J., Diagouma A., (2007), "Numerical Investigation of the behaviour of the church of Agia Triada, Drakotrypa, Greece", Advances in Engineering Software, Vol. 39/4, pp 284-300.
[34]. V.J. Soulis and G. C. Manos G.C. (2019), "Numerical Simulation and Failure Analysis of St. Konstantinos Church, after the Kozani Earthquake" International Journal of Civil Engineering (2019) 17:949–967 https://doi.org/10.1007/s40999-018-0345-5
[35] George C. Manos, Lambros Kotoulas and Evangelos Kozikopoulos "Evaluation of the Performance of Unreinforced Stone Masonry Greek "Basilica" Churches When Subjected to Seismic Forces and Foundation Settlement", Journal, buildings, Published: 30 April 2019.
[36] SAP2000, Integrated Software for Structural Analysis and Design, Computers and Structures Inc.
[37]. European Committee for Standardization, Euro-code 6 ; "Design of Masonry Structures, Part 1-1: General Rules for Building. Rules for Reinforced and Un-reinforced Masonry", EN 1996-1-1: 2005.
[38]. Manos G. C., Kotoulas L., Felekidou O, Vaccaro S. and Kozikopoulos E., (2015) "Earthquake damage to Christian Basilica Churches – Application of an expert system for the preliminary in-plane design of stone masonry piers", Int. Conf. STREMAH 2015.
[39] Provisions of Greek Seismic Code with revisions of seismic zonation", Government Gazette, Δ17α /115/9/ΦΝ275, No. 1154, Athens, 12 Aug. 2003.
[40]. European Committee for Standardization, Euro-code 8 : Design of structures for earthquake resistance - Part 1: General rules, seismic actions and rules for buildings, FINAL DRAFT prEN 1998-1, Dec. 2003.
[41]. GEER - EERI - ATC 2014. "Cephalonia GREECE Earthquake Reconnaissance January 26th/ February 2nd 2014", Report Version 1: June 6 2014.

[42] G.C Manos; E. Kozikopoulos L. Kotoulas; O. Felekidou "The earthquake performance of stone masonry Basilica churches in Kefalonia-Greece including wall detachment and soil-foundation deformability", 16 IBMAC, Padova, Italy, June 2016.
[43] Papaioannou Ch. et al., "Strong ground motion of the 3rd February 2014, (M=6.0) Kefalonia Earthquake", Institute of Earthquake Engineering and Engineering Seismology Report, Feb., 2014.
[44]. Manos G.C. & Karamitsios N., "Numerical simulation of the dynamic and earthquake behavior of Greek post-Byzantine churches with and without base isolation", Earthquake Engineering Retrofitting of Heritage Structures, Design and evaluation of strengthening techniques, pp. 171-186, Edited By: S. Syngellakis, Wessex Institute of Technology, UK, ISBN: 978-1-84564-754-4, eISBN: 978-1-84564-755-1, 2013.
[45] George C. Manos, Lambros Kotoulas and Evangelos Kozikopoulos "Evaluation of the Performance of Unreinforced Stone Masonry Greek "Basilica" Churches When Subjected to Seismic Forces and Foundation Settlement", Buildings 2019, 9, 106; doi:10.3390/buildings9050106.